DEUTSCHE GESELLSCHAFT FÜR ORTUNG UND NAVIGATION E.V.

International Radar Symposium 2009

- IRS 2009 -

09 - 11 September 2009

Hamburg, Germany

organised by:

Technical Universitv Hamburg-Harburg

TUHH

Technische Universität Hamburg-Harburg

in co-operation with

German Institute of Navigation (DGON)

This paper is accepted for oral presentation on the IRS 2009 and will appear in the conference proceedings.

V9 11.8.09

RCS - Numerical, Methodological and Conceptional Aspects for the Analysis of Radar Distorting Objects

Gerhard Greving, Wolf-Dieter Biermann, Rolf Mundt
NAVCOM Consult
Ziegelstr. 43, D-71672 Marbach
navcom.consult@t-online.de

Abstract

An increasing number of Wind turbines WT are often to be located in some distance to ground based navigation, landing and radar systems. Unacceptable distortions have to be avoided which harm the mission of these systems. The most critical systems are the radar systems.
For the safeguarding task, the Radar Cross Section RCS is often used to determine the threat and to analyze distorted parameters. The RCS is a normalized scattering parameter. It is shown in this paper that the RCS does not exist for the WT being installed on the ground due to fundamental reasons.
Methodological numerical examples are presented for the scattering of generic metallic plates, showing the "caustic problem" for the GTD/UTD-method and spatial under-sampling effects in the graphical results.
The use and relevance of the RCS is discussed for the evaluation of the False Target Reports FTR for the Primary Air Traffic Control Radar PSR ATC.
Multi-scattering cases are studied for a large WT (E82) and an average medium aircraft B737-800. It is concluded that FTR are extremely unlikely and unrealistic to occur.

Introduction

Often building activities are planned close to a radar site. The radar can be an Air Traffic Control ATC, air defense or weather radar. These objects may distort or harm the operation of the radar. It has to be evaluated in advance if the planned objects, such as wind turbines or hangars or terminals, will harm the operation of the radar system in a way that the assigned mission of the radar cannot be maintained sufficiently. However, it is often not uniquely clear which kind and level of "distortion" harms the radar in a way that the mission cannot be done. It is not clear often due to the lack of agreed standardized specification if an effect is an un-acceptable distortion or a discomfort for the radar controller. It should be also common sense that a status of "no distortion" or "no risk" or "100% safety" cannot be achieved at all - even in the absence of man-made distorting objects such as the wind turbines WT. This paper continues the series of papers of the authors [6-11] for the methodology and the numerical evaluation of WT in the radiation field of radar. A particular continued first topic is the methodology of the simulation of the RCS for the WT on the ground. A second topic studies the potential generation of FTR for the primary Air Traffic Control Radar PSR by a multi-scattering at the WT and A/C [12] as proposed by the adapted RCS application in the common well known radar equation [2, 3,].

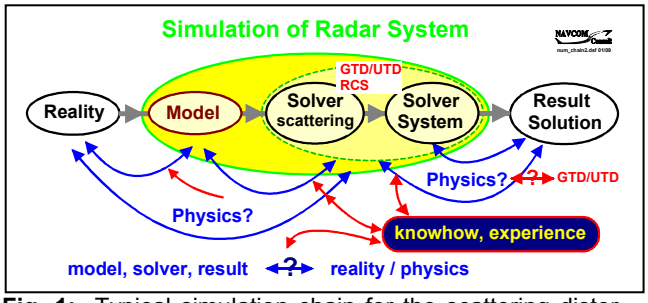

Fig. 1: Typical simulation chain for the scattering distortions of a radar system. GTD/UTD methods (potentially) used in the solver step for the RCS

Basics of the RCS and Radar Equation; Wind Turbines

It is often tried and proposed to apply the RCS for the safeguarding tasks of the radar and sometimes also for other systems regarding wind turbines naturally installed on the ground. The RCS is by that part of the simulation chain for the determination of the performance of the radar. Many errors can occur in such a simulation process as shown in Fig. 1.

The following equation (1) shows the well known radar equation [2] where the RCS σ is a factor which should characterize the target. From (1) follows directly the maximum range equation [2, 3]

$$P_r = \frac{P_t G_t G_r \sigma \lambda^2 F_t^2 F_r^2}{(4\pi)^3 R^4} \qquad (1)$$

Equation (2) shows the standard unique definition of the RCS [1-4]

$$\sigma_{pq} = \lim_{R\to\infty}\left[4\pi R^2 \frac{\left|E_p^s\right|^2}{\left|E_q^i\right|^2} \right] \qquad (2)$$

The fundamental obligatory limit condition R→∞ implies a plane wave excitation as explained also in the IEEE definition of terms [1]. The infinite distance may be substituted practically and approximately by the far field condition [2-4].
The plane wave is characterized by a constant amplitude and by a linearly progressing phase across the object. This basic condition and fundamental requirement is simply not given in the case of an object on the ground and by that the RCS is not defined for objects on the ground. The natural consequence is that all tools for the RCS require the inherent plane wave source and in the measurements a plane wave has to be approximated. A ground plane is rejected thereof in the RCS calculation of serious tools.
The authors have outlined in several publications [6-11] the basic and principal non-applicability of the RCS-scheme for objects on the ground, such as WT. The simple application of the RCS in the radar equation cannot be a justification for the application of the RCS for WT. The RCS cannot be also an approximation in the case of the WT, because first ***no unique RCS-figure*** exists at all for a WT as shown again below for the WT also in free space and, second, the error made is unpredictable. One could take just the "maximum RCS" or just some large figure in the sense of a "worst case". Worst case ideas may be generally on the safe side for the systems, but are arbitrary and unjustified in the case of the WT because this procedure penalizes the acceptance of the WT by problematic unjustified large safeguarding distances. For typical distances in question for safeguarding, the WT are by far not in the mutual far-field of the PSR-ATC-radar and the WT and the A/C are by far not in their mutual far-field as well. In the typical distance of 5000m, the phase error is up to about 3960deg instead of the permitted 22.5deg for the WT.
It should be re-iterated that the so-called "near field RCS" is not a new additional definition and a new quantity of an RCS figure, but only the same RCS determined by near field quantities. No new boundary conditions apply. This "near field scheme" also does not modify the requirement of the basic infinite distances in the definition of RCS.
However, this paper shall give in the following first chapter some detailed theoretical and numerical results for the simulation of the RCS and discusses hereafter the problematic application of the RCS in the course of the determination of FTR in the scenario of the ATC-S-band radar and WT and A/C.

RCS and Numerical Methods; Artifacts

The mono-static and bi-static RCS is a field quantity (2) [1-4], normalized to the incident field.
In principal, every suitable and applicable numerical analysis method can be used for the RCS. However, as shown in Fig. 1, the methods must be correctly applied and must reflect the physical process. A widely applied method is the GTD/UTD-method (Geometrical/Uniform Theory of Diffraction) which reacts in certain situations problematically, i.e. the problem of the well known "caustic" [3] as shown. The GTD/UTD-method is simply not applicable in this region. Such kinds of effects have to be expected if objects are composed of plates.

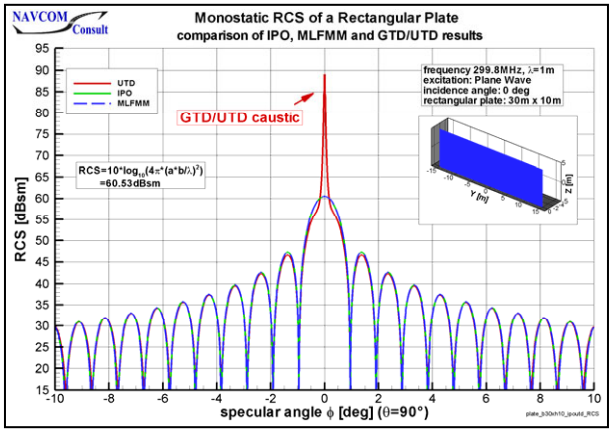

Fig. 2: Mono-static RCS of a simple generic metallic rectangular plate for 3 numerical methods (IPO, MLFMM and GTD/UTD)

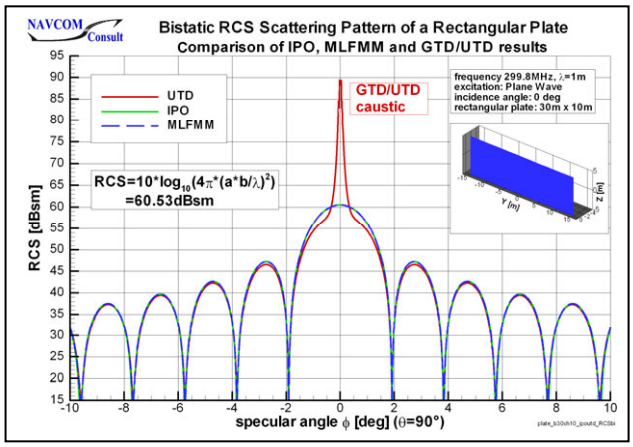

Fig. 3: Bi-static RCS of the same plate of Fig. 2

Fig. 2 shows the mono-static RCS of an electrically large metallic rectangular plate (30λ*10λ) calculated by 3 different numerical methods: GTD/UTD, IPO (Improved Physical Optics) and the MLFMM (iterative version of the rigorous method of moments MoM). It can be clearly seen that the GTD/UTD solution exhibits a large unphysical peak which is about 30dB larger than the two other solutions which are in good agreement. This unphysical peak is an artifact and occurs in the region of the symmetry axis for the mono-static case and in the region of the main reflection in the bi-static case (Fig. 3).
This generic plate is a simple case and the peak is obvious. But in complex cases the "caustic problem" may not be so apparent and the artifact(s) may not be discovered easily in GTD/UTD solutions.

For a second larger metallic plate (60λ*60λ; Fig. 4), the artifact can be seen as well for the GTD/UTD solution. But in the IPO-case, 2 angular resolutions have been presented, one high resolution and one low resolution by angular steps of 1deg. In the latter case, an apparent and non-existing peak like behavior can be seen in the direction of the main reflection where the GTD/UTD solution itself exhibits the "caustic problem". The peak-effect for IPO is just due to the spatially insufficient angular sampling, i.e. a pictorial "under-sampling" phenomenon (see also examples in [5]) and not a "caustic problem". All calculated RCS figures are correct.

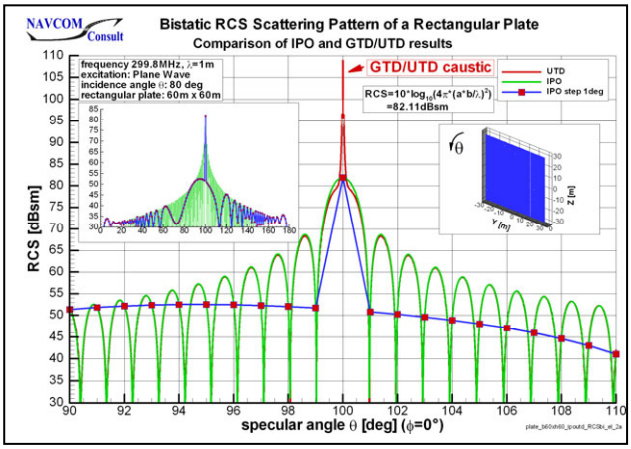

Fig. 4: Bi-static RCS of a large metallic plate; 2 methods: "caustic problem" for GTD/UTD, undersampling for IPO

RCS, Wind Turbines and FTR; Statistical Approach

"False Target Reports" FTR are one of the discussed potential distortion modes of primary S-band ATC-radar PSR by WT [12]. The RCS and radar equation scheme is proposed and, by that, has been studied pro forma in the following by systematic statistical RCS calculations and evaluations *regardless that the RCS is not applicable for the WT on the ground*.

Two proposed purely theoretical types of FTR for a PSR may be possible in principle as shown in Fig. 5 and Fig. 6:

- "additional A/C" in the direction of the WT In this case the main beam of the 2D-radar points to the WT and a double bi-scattering at the WT and mono-static scattering at the A/C takes place. Obvious that a false target can be detected in the radar only, if enough back-scattered signals appear in the radar receiver.
- "additional WT" in the direction of the A/C . In this case the main beam of the 2D-radar points to the A/C high up in space and a double bi-scattering at the A/C and a mono-static scattering at the WT on the ground takes place.

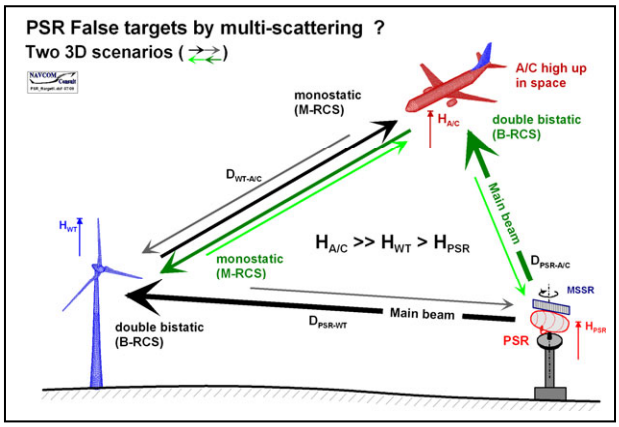

Fig. 5: General scenario of PSR FTR by multi-scattering

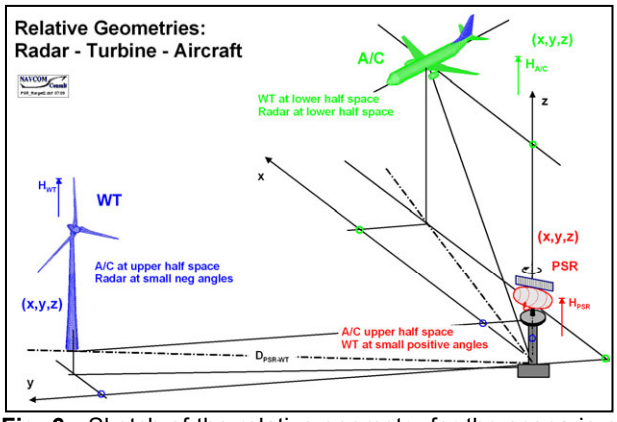

Fig. 6: Sketch of the relative geometry for the scenario of radar, WT and A/C

Other theoretically possible multi-scattering paths via the radar sidelobes are ruled out a-priori as to be fully practically unrealistic and are not discussed assuming a practical real high performance sidelobe suppression of 30dB minimum.

$$P_r = \frac{\sigma_{A/C}\sigma_{WT1}\sigma_{WT2}F_{rWT}^2F_{tWT}^2G_rG_t\lambda^2}{(4\pi)^5 D_{PSR-WT}^4 D_{WT-A/C}^4} \qquad (3)$$

The adapted radar equation (3) is proposed [12] for the case in Fig. 5 where the radar points to the WT. Due to reciprocity it holds $\sigma_{WT1}=\sigma_{WT2}$ and the pattern factors F are equal as well because the transmit and receive antennas are the same, and reciprocity applies as well.

These two scenarios (Fig. 5) are characterized and bounded by some facts, that

- the acceptable minimum distance of the WT to the ATC-radar is bounded by other conditions (e.g. shadowing) and by that the distance between the WT and A/C is bounded as well.
- the upper half space for the effective appearance of the A/C relative to the WT is restricted due to operational constraints, e.g. >+5° in elevation for close distances. But the A/C can be in the remaining full upper half space.

- the A/C is generally much higher than the radar and the WT – at least in the only relevant short distances. By that, the WT as well as the radar are relevant for the RCS of the A/C only in the lower half space above some minimum elevation angle.
- The WT or at least the hub and tip are higher than the radar and the illumination of the WT by the radar is restricted to a small angular region, e.g. ±2°.

Basics of the numerical simulation of the RCS

In this paper, the mono-static and bi-static RCS is calculated for the WT and the A/C by the numerical method IPO (Improved Physical Optics). It is in fact an improved and extended PTD-method (Physical Theory of Diffraction). The GTD/UTD method has not been taken due to the discussed reasons.
For the WT, the ground is neglected physically fully unjustified due to the discussed (formal) reasons. Both RCS-types are needed in the relevant spatial volumes relative to the WT and the A/C.

RCS of the WT Enercon E82

A large modern WT (Enercon E82; power range of 2-3MW) has been modelled by a very large number of metallic triangular patches (Fig. 7) in the S-band. Also the blades are modelled fully metallic in a worst case sense, by that taking into account water and ice effects.
It is obvious that these simulations require extreme computer resources. Due to that, only some numerical results are shown in this paper. More will be shown on the conference itself.

The bi-static RCS of the E82 has been numerically calculated in the elevation volume from 0° to 40° and in the full azimuth range (Fig. 8).

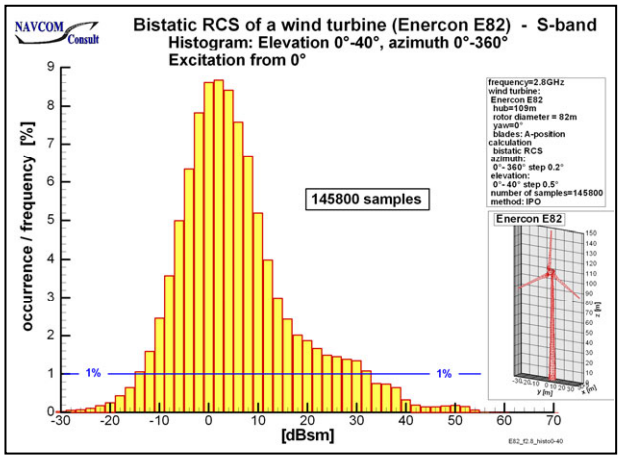

Fig. 8: Example: Statistics of the bi-static RCS of an E82 in the lower half space down to -40° elevation

In total, 145800 samples have been calculated and evaluated in the shown histogram. The histogram

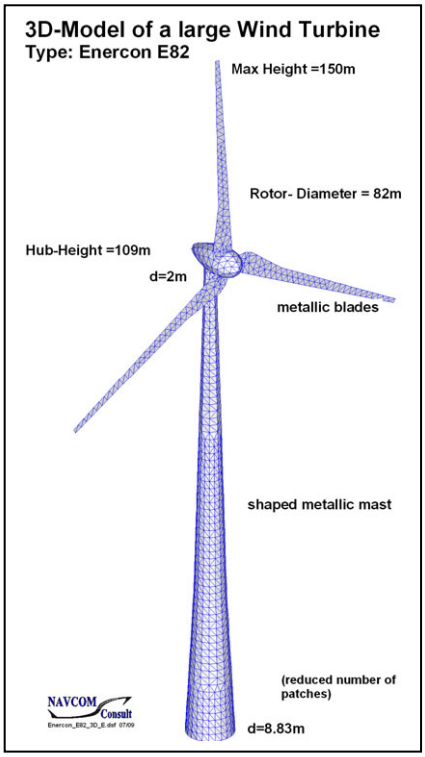

Fig. 7: 3D model of a large modern WT Enercon E82

shows the statistical occurrence and distribution of the individual RCS figures, but also enables the determination of the absolute occurrence by the noted calculated maximum total number of samples.
It can be seen clearly that the large RCS (e.g. >40dBsm) are very rare. The 1% limit is at about 32dBsm. The largest number of bi-static RCS are in the range between -5dBsm and +10dBsm. The peak is at +2dBsm. If the elevation angle would be increased, the peak tends to move to lower values and the percentage is increasing. Statistically, the larger figures are less and less significant then.

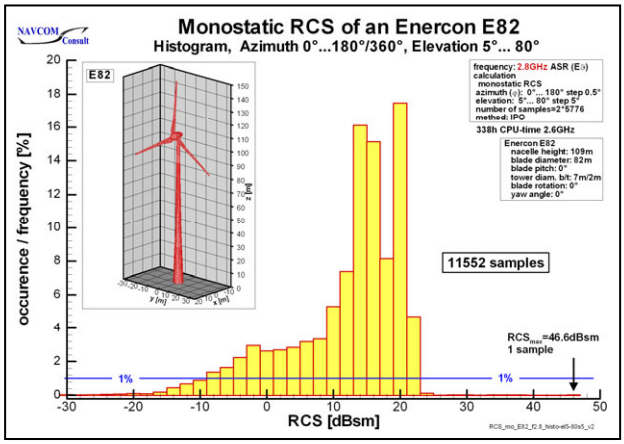

Fig. 9: Example: Statistics of the mono-static RCS of an E82 at samples in the upper half space above 5° elevation

Fig. 9 shows an example of the statistics of the mono-static RCS of the E82 in the relevant upper half space >+5° up to +80°. The vast majority of mono-static RCS is below 22dBsm. The maximum

mono-static RCS of +77.6dBsm has been calculated for a small positive elevation angle which is irrelevant in the discussed ATC-scenarios. This high value is related to the metallic blade model and will not appear in reality with a relevant probability. More results will be shown on the conference itself.

RCS of the A/C B737-800

The aircraft B737-800 has been chosen for the study and has been modelled (Fig. 10) because it may cover the majority number of the typical aircraft flying in space, such as the A318-A321, the smaller B757 and all the large number of smaller aircraft and the commuter and general aviation A/C.

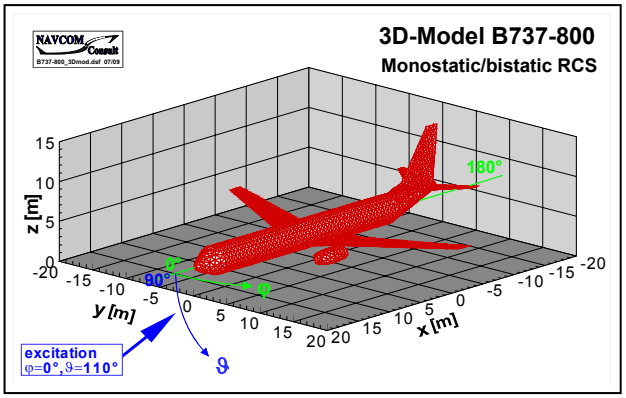

Fig. 10: 3D model of an aircraft B737-800

Wide body aircraft will certainly have larger maximum RCS-values and a higher average value in the statistics. However, the principal behaviour of the statistics will remain that large RCS figures are possible but rare. It does not seem to be justified to consider in this statistical evaluation a cascaded worst-case scenario, namely the rare worst case RCS somewhere in space as well as the worst case A/C etc. This again seems to be a reasonably not existing over-exaggeration of the potentially threatening effects by the WT.

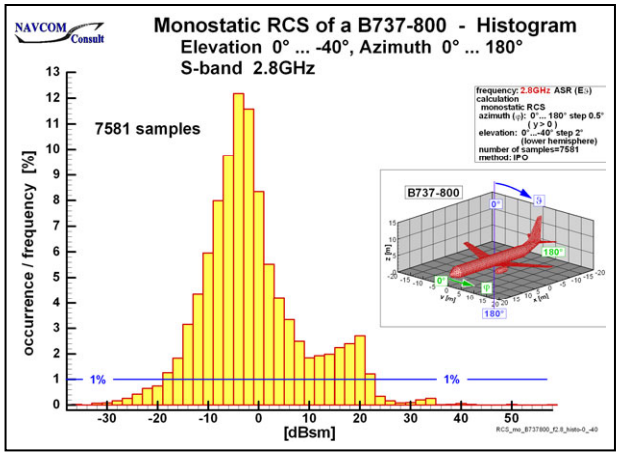

Fig. 11: Example: Statistics of the mono-static RCS of a B737-800

The mono-static and bi-static RCS have been calculated in the lower half space (Fig. 10) down to the elevation -40° (ϑ=130°). 7581 samples have been calculated and statistically evaluated by a histogram for the mono-static case (Fig. 11 and Fig. 12) and in total 570790 samples for the bi-static case (Fig. 13).

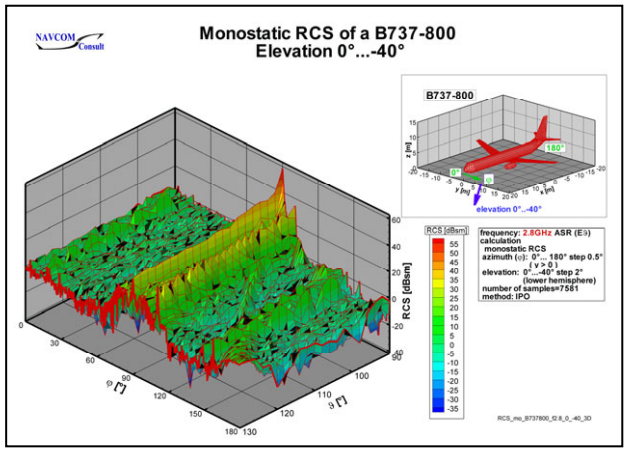

Fig. 12: 3D display of the mono-static RCS function of a B737-800 of Fig. 10 (Note: elevation=0° equals ϑ=90°)

Fig. 12 shows all the calculated mono-static RCS-functions in 3D. The (relative) maximum appears orthogonal to the fuselage in each RCS-function as expected. The largest mono-static RCS is >50dBsm, but only one time of the 7581 samples calculated. About 99% of the RCS-figures are below 23dBsm and the majority is around 0dBsm. This histogram will not change significantly by the inclusion of the rest of the lower half space. Only about 1% of the RCS have an amplitude of about 22dBsm.
In the bi-static case, 9 incidence angles of the plane wave have been defined and for each incidence angle the truncated lower half space has been sampled sufficiently. In total, 570790 samples have been calculated and evaluated (Fig. 13).

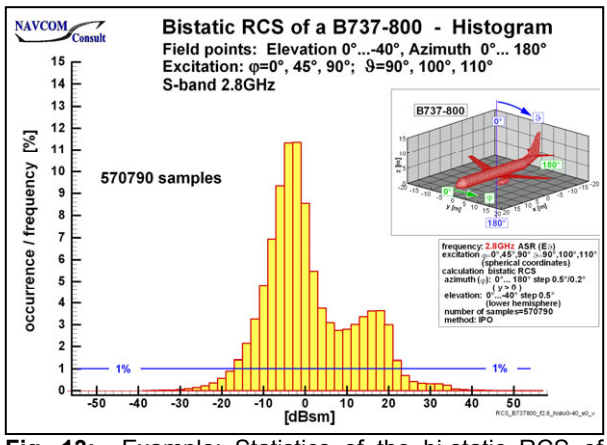

Fig. 13: Example: Statistics of the bi-static RCS of a B737-800

The statistical behaviour of the bi-static RCS is similar to the mono-static case. 99% of the bi-static RCS are below about 24dBsm. Only about 1% of the

RCS have an amplitude of about 23dBsm. It is not expected that the histograms (Fig. 11, Fig. 13) will change significantly for the complete lower half space.

Application of the RCS results to the PSR FTR

The statistical histograms of the WT (E82) and of the A/C (B737-800) allow the quantitative and qualitative evaluation of the potential existence FTR in the multi-scattering environment by the PSR radar, WT and A/C. It is anticipated and can be easily shown that for relevant distances of the WT to the PSR and of the A/C to the WT, an FTR can be created only for the ***simultaneous statistical existence of the very rare large RCS-figures*** for the WT as well as for the A/C. This is extremely unlikely to occur as has been shown.
E.g., if one assumes a spatially unrealistically constant worst case RCS-figure of 40dBsm for the WT as well as for the A/C, an exaggeration of more than 40dB can be found easily for more than 99% of the two discussed cases (Fig. 5). For the typical upper average figures of the mono- and bi-static RCS for the WT and A/C, an exaggeration of more than 60dB can be found. For larger aircraft, only the partial figures for the A/C change.
This fictive discussion assumes that the RCS is applicable for the WT – but, it is not as discussed above.

In addition, the following facts will even ***decrease*** the probability of the ***existence*** of the FTR for a PSR created by a WT, e.g. :

- The ground reduces the scattering at the WT.
- The finite near field distance between the radar and the objects and mutually between the objects reduces the scattering significantly.
- The required relevant short distances between the A/C and the WT for an FTR are limited by operational means in a normal aviation situation for relevant airliners. It is un-technical and operationally un-realistic to assume extreme short distances and low heights (<500m distance, <200m height).

Summary

The RCS has been discussed first in the context of the application of numerical methods. It has been shown that unphysical RCS-figures can occur in case of the widely used GTD/UTD method, namely the “caustic type effects”. It has been shown also that an adequate spatial sampling of the RCS should be applied in order to avoid mis-interpretations of the RCS-results.
It has been shown again, that the RCS-scheme is generally not applicable for objects on the ground such as WT. In the discussed multi-scattering cases near-field effects reduce the scattering drastically further on compared to the RCS concept.
Potential false targets by multi-scattering have been studied by systematic statistically sufficient sampling of the relevant volumes. It can be concluded that only in extremely rare and unrealistic cases an FTR may be produced by the discussed multi-scattering at the WT and the A/C. Among the two cases (Fig. 5) the one is the more relatively unlikely one where the radar points to the WT. FTR cannot be generated by multi-scattering cases in reality for realistic scenarios and taking into account the statistical RCS-figures where the sidelobes of the radar are involved.

Acknowledgments

Valuable comments by Dr. N. Zhu (University of Stuttgart) and technical discussions are grateful appreciated.

References

[1] IEEE STD 211-1997, Definition of terms
[2] SKOLNIK Radar Handbook, McGraw Hill, Boston 1990
[3] LO, LEE Antenna Handbook I, Chapman&Hall, NewYork 1993
[4] KNOTT et.al. Radar Cross Section, Artech House, Boston 1993
[5] RIGLING B.D. and R. L. MOSES R.L. GTD-based scattering models for bistatic SAR,” in Algorithms for Synthetic Aperture Radar Imagery XI, E. G. Zelnio, ed., Proceedings of SPIE 5427, pp. 208–219, 2004.
[6] GREVING G. Numerical Analysis of the effects by scattering from objects on ATC-radar and various methods for its reduction - Theory, results, IRS 2006, Krakow/Poland
[7] GREVING G. Numerical Simulations of Environmental Distortions by Scattering of Objects for the Radar - SSR and flat roofs, RCS and windturbines, EURAD 2006, September 2006 Manchester/UK
[8] GREVING G., BIERMANN W.-D, MUNDT R. Wind Turbines and Radar - The Radar Cross Section RCS a Useful Figure for Safeguarding? IRS 2007, September 2007 Cologne/Germany
[9] GREVING G., BIERMANN W.-D. Application of the Radar Cross Section RCS for Objects on the Ground - Example of Wind Turbines, IRS 2008, Wroclav/Poland, May 2008
[10] GREVING G., BIERMANN W.-D, MUNDT R. Status of Advanced Scattering Distortion System Analysis for Navaids and Radar - Examples of A380 and Wind Turbines; MRRS 2008, September Kyiv/Ukraine 2008, (Invited Paper)
[11] GREVING G., BIERMANN W.-D, MUNDT R. On the Relevance of the Measured or Calculated RCS for Objects on the Ground - Case Wind Turbines; EUCAP 2009, Berlin March 2009
[12] EUROCONTROL; Guidelines on How to Asses the Potential Impact of Wind Turbines on Surveillance Sensors; Ed. 0.14, 17.6.09